

# Macro and Microscopic CH<sub>4</sub>–CO<sub>2</sub> Replacement in CH<sub>4</sub> Hydrate Under Pressurized CO<sub>2</sub>

Masaki Ota, Takeomi Saito, Tsutomu Aida, Masaru Watanabe, Yoshiyuki Sato,  
Richard L. Smith Jr., and Hiroshi Inomata

Research Center of Supercritical Fluid Technology, Dept. of Chemical Engineering, Tohoku University,  
Aoba-ku, Sendai 980-8579, Japan

DOI 10.1002/aic.11294

Published online August 30, 2007 in Wiley InterScience (www.interscience.wiley.com).

*CH<sub>4</sub>–CO<sub>2</sub> replacement in CH<sub>4</sub> hydrate with high pressure CO<sub>2</sub> was studied with in-situ laser Raman spectroscopy at 273.2 K and at initial pressures of 3.2, 5.4, and 6.0 MPa. Replacement rates increased with increasing pressures up to 3.6 MPa and did not change at higher pressures (~6.0 MPa). These results showed that the replacement rates were dependent on pressure and phase conditions with the driving force being strongly related to fugacity differences of the two guest components between fluid and hydrate phases. When CH<sub>4</sub> hydrate was contacted with CO<sub>2</sub> under flow conditions, in-situ Raman measurements of the hydrate phase showed differences of cage decomposition rates between the Medium-cage (M-cage) and the Small-cage (S-cage) in the CH<sub>4</sub> hydrate with decomposition of the M-cage being faster than that of the S-cage. The van der Waals–Platteeuw model was applied to the measurements of the transient data and it is shown that the theory allows estimation of occupancies of each component during replacement. © 2007 American Institute of Chemical Engineers AICHE J, 53: 2715–2721, 2007*

**Keywords:** CH<sub>4</sub> hydrate, CO<sub>2</sub> hydrate, replacement mechanism, Raman, cage

## Introduction

Natural gas hydrate, CH<sub>4</sub> hydrate, forms under conditions of low temperatures and high pressures and exists naturally below the ocean floor or in the permafrost zones.<sup>1</sup> One method for CH<sub>4</sub> recovering that has been proposed is by replacement with condensed CO<sub>2</sub>.<sup>2</sup> In this method, CH<sub>4</sub> is recovered from CH<sub>4</sub> hydrate by replacement with CO<sub>2</sub> and thus CO<sub>2</sub> can possibly be sequestered under the sea bed. The advantage of such a process is that the CO<sub>2</sub> can be expected to stabilize the ocean floor during the methane recovery because CH<sub>4</sub> hydrate and CO<sub>2</sub> hydrate form the same structure (sI) hydrate whose unit cell consists of six medium cages (M-cage) and two small cages (S-cage).<sup>1</sup>

Several researchers have examined whether the replacement might occur in CH<sub>4</sub> hydrate using pressurized CO<sub>2</sub> on

a laboratory scale.<sup>2–9</sup> Measurements of hydrate–liquid–vapor (H–L–V) equilibria in the CH<sub>4</sub>–CO<sub>2</sub>–H<sub>2</sub>O system show that CO<sub>2</sub> hydrate is thermodynamically more stable than CH<sub>4</sub> hydrate at temperatures below 283 K, because the equilibrium pressures of CO<sub>2</sub> hydrate are lower than those of CH<sub>4</sub> hydrate.<sup>2</sup> The distribution coefficient of CH<sub>4</sub> and CO<sub>2</sub> between the gas and the hydrate phase measured at 280 K show that CO<sub>2</sub> distributes in the hydrate phase relative to CH<sub>4</sub>.<sup>3</sup> Further, Gibbs free energy for the replacement is negative and thus the process is theoretically spontaneous.<sup>4</sup> Hirohama et al. demonstrated that dynamic replacement was feasible and showed that the replacement occurred in the presence of liquid CO<sub>2</sub> at 274 K and 3.6 MPa.<sup>5</sup> It has been suggested that CH<sub>4</sub>–CO<sub>2</sub> replacement occurs under conditions of 275 K and 2.0 MPa<sup>6</sup> and 278 K and 3.0 MPa<sup>7</sup> in gaseous–hydrate reactions.

A number of proposals have been made concerning the replacement mechanism.<sup>5,8,9</sup> Hirohama et al. implied that the driving force for the replacement is the fugacity difference of

Correspondence concerning this article should be addressed to M. Ota at masao@scf.che.tohoku.ac.jp.

two guest molecules between the fluid and the hydrate phases.<sup>5</sup> In our previous studies, we proposed a film diffusion model for the replacement considering the driving force as fugacity differences, which could describe the time evolution of the replacement.<sup>8,9</sup> Analysis of the activation energies shows that after the surface reaction at the beginning of the replacement process, the CH<sub>4</sub> hydrate decomposition is dominated by rearrangement of the water molecules in the hydrate, and CO<sub>2</sub> hydrate formation is dominated by diffusion in the hydrate phase.<sup>8</sup>

In the literature, the range of the experimental conditions, especially pressure conditions, are still limited to pressures below 3.6 MPa, corresponding to a depth in the sea of ~360 m. As CH<sub>4</sub> hydrate exists mainly below a depth of 500 m, further investigation of pressure conditions are needed to discuss possible pressure effects on the replacement mechanism. Increasing pressure of the fluid phase is expected to increase the replacement rates, because the individual hydrate growth can be promoted with pressure.<sup>10,11</sup> Hence, a study that examines replacement rates at different pressures would allow one to clarify the relationships for fugacity difference driving force with the goal to develop an overall strategy for the efficient replacement of CH<sub>4</sub> with CO<sub>2</sub> for large undersea hydrate beds. In this work, we studied the macroscopic replacement of CH<sub>4</sub> with CO<sub>2</sub> for given fugacity and phase conditions. Kinetics of the replacement was examined quantitatively by following the time evolution of CH<sub>4</sub>/CO<sub>2</sub> ratios in the fluid and hydrate phases in batch experiments.

In a previous report, the microscopic mechanism of replacement in CH<sub>4</sub> hydrate was studied with an in-situ Raman technique.<sup>9</sup> Analysis of the Raman spectra for CH<sub>4</sub> hydrate showed that replacement could be divided into two regions indicating the M-cage and the S-cage,<sup>12</sup> and that the replacement rates were different between M-cage and S-cage of CH<sub>4</sub> hydrate with the cage decomposition in the M-cage proceeding faster than that in the S-cage. Similar trends have been observed in CH<sub>4</sub>-CO<sub>2</sub> replacement reactions using the solid state NMR.<sup>13</sup> This difference in cage decomposition rates was probably related to the stability of the cage structures between M-cage and S-cage and the energetic stability of guest molecule occupation in the each cage.

From these measurements, we proposed a kinetic model that included cage decomposition on the microscopic replacement,<sup>9</sup> which was based on the stoichiometric analysis of CO<sub>2</sub> occupied in M-cage and CH<sub>4</sub> reoccupied in S-cage. We assumed a ratio of 3 as a stoichiometric constant due to the theoretical cage number (M-cage:S-cage = 6:2) in a unit cell. This constant, however, exhibited a time dependence, which was close to this assumed value in the initial stages of the experiment, but deviated from the value as time progressed. Hence, the microscopic mechanism still has interesting points that need further investigation.

In this work, we also studied the microscopic replacement of CH<sub>4</sub> hydrate with CO<sub>2</sub> by conducting in-situ measurements of cage decompositions in the CH<sub>4</sub> hydrate using a laser Raman technique in a flow system. We apply the van der Waals-Platteeuw theory<sup>1,14</sup> to the experimental data obtained in the former batch experiments and evaluate the rate differences in the cage decomposition for M-cage and S-cage in CH<sub>4</sub> hydrate under progressively higher CO<sub>2</sub> pressures. Through discussion, we examine the possibility of

adapting the theory to the replacement reactions and discuss the microscopic replacement mechanism from available data.

## Materials and Methods

### Materials

CH<sub>4</sub> (99.9 %) and CO<sub>2</sub> (99.5 %) were supplied by Nippon Sanso without further purification. Distilled/deionized water (electric conductivity, 5.5  $\mu$ S/m) was obtained from a water distillation apparatus (Yamato, WG-221).

### Experimental apparatus

Details of the experimental apparatus are described elsewhere.<sup>8</sup> The experimental apparatus consisted of a high pressure view cell with internal volume of 129.8 cm<sup>3</sup> (AKICO), a feed system, a back pressure regulator, cooling system (ADVANTEC, LE-600), and a laser Raman spectrometer (JASCO, NRS2000). The view cell had three diametrically opposed optical windows, which allowed 90° and 180° Raman scattering measurements. The apparatus was used for both batch and flow experiments.

### Preparation of CH<sub>4</sub> hydrate in high-pressure optical cell

The method of CH<sub>4</sub> hydrate preparation for batch and flow experiments was essentially the same as used in our previous study.<sup>8</sup> CH<sub>4</sub> hydrate was formed by mixing water with CH<sub>4</sub> gas using magnetic drive screw type agitation inside the cell at 273.2 K and the pressure above the three-phase equilibrium pressure of CH<sub>4</sub> hydrate at this condition. Agitation of ~100 rpm was performed for 24 h to promote CH<sub>4</sub> hydrate formation. The obtained average occupancy was 0.93 that was determined by gravimetric and pressure change methods in each of the experiments. The formation of CH<sub>4</sub> hydrate was confirmed by the Raman analysis. Table 1 shows the conditions used in the replacement experiments. The loaded amount of water was measured gravimetrically and the initial moles of CH<sub>4</sub> in the hydrate phase were calculated with material balance using the volume expansion method used in the previous study.<sup>8</sup>

### Experimental procedures

*Batch Experiments (Runs 1, 2, and 3).* After preparing the CH<sub>4</sub> hydrate, CH<sub>4</sub> in the gas phase was purged by high pressure CO<sub>2</sub> (gaseous or liquid) until CH<sub>4</sub> was completely replaced with CO<sub>2</sub> in ~20 min, which was confirmed by the disappearance of the Raman peak of CH<sub>4</sub> in the CO<sub>2</sub>-rich phase. The existence of CH<sub>4</sub> hydrate was also checked simultaneously with the Raman analysis. The replacement reaction started when the cell was set to the target pressure of 3.26, 5.40, or 6.00 MPa. The reaction was followed at the boundary of gaseous and hydrate phase at 3.26 MPa (Run 1) and that at the boundary of liquid and hydrate phase at 5.40 and 6.00 MPa (Runs 2 and 3).

In the gaseous-hydrate replacement (Run 1), the compositions of gaseous mixtures were determined by Raman analysis,<sup>8</sup> and the density was calculated with the Trebble-Bishnoi equation of state<sup>15</sup> at the experimental conditions of temperature and pressure. This procedure allowed us to follow the time evolution of amounts of the gas phase at desired inter-

**Table 1. Experimental Conditions for CH<sub>4</sub>–CO<sub>2</sub> Replacement Experiments**

	$P_{\text{initial}}$ (MPa)	Loaded Water (mmol)	Initial Moles of CH <sub>4</sub> in the Hydrate Phase (mmol)	Time (h)	Reaction Type
Run 1	3.26	1150	197	285	Batch
Run 2	5.40	1790	248	64	Batch
Run 3	6.00	1160	196	260	Batch
Run 4	3.20	1120	190	280	Flow

Temperature for all runs was 273.2 K.

vals, and as a consequence, it was possible to determine the amount of CH<sub>4</sub>/CO<sub>2</sub> hydrates by subtracting the amounts of these components initially introduced into the cell from those in the gas phase.<sup>8</sup> After a given time, hydrate mixtures were completely decomposed by heating to check the material balance. The compositions and densities of the obtained gaseous phase were analyzed using Raman spectroscopy and the Trebble–Bishnoi EOS, respectively. For those runs, the material balances of CH<sub>4</sub> and CO<sub>2</sub> before and after reaction were found to be 101% for CH<sub>4</sub> and 90% for CO<sub>2</sub>.

In the liquid–hydrate replacement experiments (Runs 2 and 3), we chose a simple method to quantify the CH<sub>4</sub>–CO<sub>2</sub> hydrate mixtures. Hydrate mixtures were decomposed by heating, and the amount of obtained gaseous phase was analyzed using the Raman spectroscopy with densities being calculated by the Trebble–Bishnoi EOS. This method was chosen since Raman spectroscopy could not distinguish between CO<sub>2</sub> in the gas and liquid phase when three phases (vapor–liquid–solid) appeared during replacement. With the methods used, the material balances of CH<sub>4</sub> and CO<sub>2</sub> were found to be in the range of 97 to 107% for CH<sub>4</sub> and 97 to 99% for CO<sub>2</sub>.

**Flow Experiments (Run 4).** After preparing CH<sub>4</sub> hydrate and successive purgings of CH<sub>4</sub> gas in the cell with CO<sub>2</sub>, the replacement reaction was followed at a set initial pressure of 3.20 MPa (Run 4). During the reaction, Raman spectra of CH<sub>4</sub> hydrate were acquired at given intervals as CO<sub>2</sub> was flowed through the cell at ~100 ml/min to eliminate the gaseous CH<sub>4</sub>. After 280 h passed, the hydrate mixtures were completely decomposed to check the replacement rates. The composition of obtained gas phase measured by the Raman analysis, corresponding to the composition of hydrate phase, were 0.69 for CH<sub>4</sub> ( $h_{\text{CH}_4}$ ) and 0.31 for CO<sub>2</sub> ( $h_{\text{CO}_2}$ ) in hydrate phase at 280 h, and these values were almost coincident with the corresponding conditions of Run 1 at 277 h in the batch experiment ( $h_{\text{CH}_4}$ : 0.73;  $h_{\text{CO}_2}$ : 0.27).

## Results and Discussion

### Quantitative analysis of CH<sub>4</sub>–CO<sub>2</sub> replacement in the hydrate phase (Runs 1, 2, and 3)

Figures 1a, b show how the composition of each component in the hydrate phase on a water-free basis changed with time at 273.2 K for the given pressures. The data of the previous study<sup>9</sup> conducted at 273.2 K and 3.60 MPa are also shown in the figures.

In Figures 1a, b, CH<sub>4</sub> mole fraction of the hydrate phase decreased with increasing CO<sub>2</sub> mole fraction at the each

pressure. The replacement reaction was promoted with increasing pressures up to 3.60 MPa, while they hardly changed above 3.60 MPa, which can be explained as follows. The replacement reaction at 3.26 MPa probably occurred at the gas–hydrate interface, while the replacement at higher pressures probably occurred at the liquid–hydrate interface. This means that the replacement system was affected by the fugacity of the fluid phase.

The fugacities of each component in fluid and hydrate phases during replacement were plotted as shown in Figure 2. Here, CH<sub>4</sub> and CO<sub>2</sub> fugacities in the fluid phase ( $f_{\text{CH}_4,\text{f}}$  and  $f_{\text{CO}_2,\text{f}}$ ) were calculated with the Soave–Redlich–Kwong equation of state (SRK-EOS)<sup>16</sup> at the experimental temperature, pressures, and compositions of fluid phase. CH<sub>4</sub> and CO<sub>2</sub> fugacities in the hydrate phase ( $f_{\text{CH}_4,\text{h}}$  and  $f_{\text{CO}_2,\text{h}}$ ) were determined from the CSMHYD program<sup>1</sup> including the van der Waals–Platteeuw theory<sup>14</sup> and the SRK-EOS for the equilibrium fugacity at the given temperature and measured hydrate composition.

In Figure 2b, the  $f_{\text{CO}_2,\text{f}}$  at 3.26 MPa decreased with time, while that at 5.40 and 6.00 MPa showed little variation

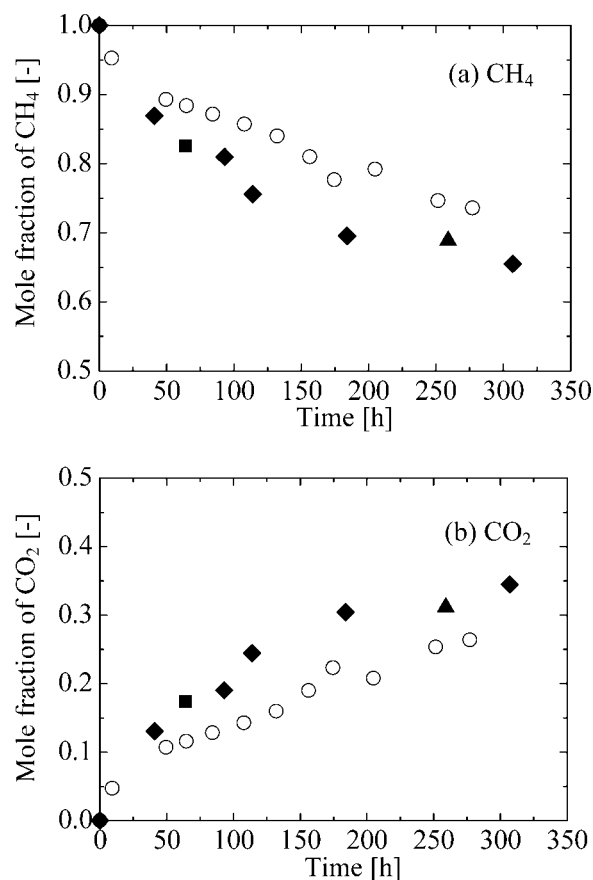


**Figure 1. Compositions of the hydrate phase (water-free) during the replacements in batch experiments as a function of time at 273.2 K and initial pressures of 3.26 MPa (circles), 5.40 MPa (squares), 6.00 MPa (triangles), and 3.60 MPa (diamonds) by Ref. 9: (a) CH<sub>4</sub>, (b) CO<sub>2</sub>.**

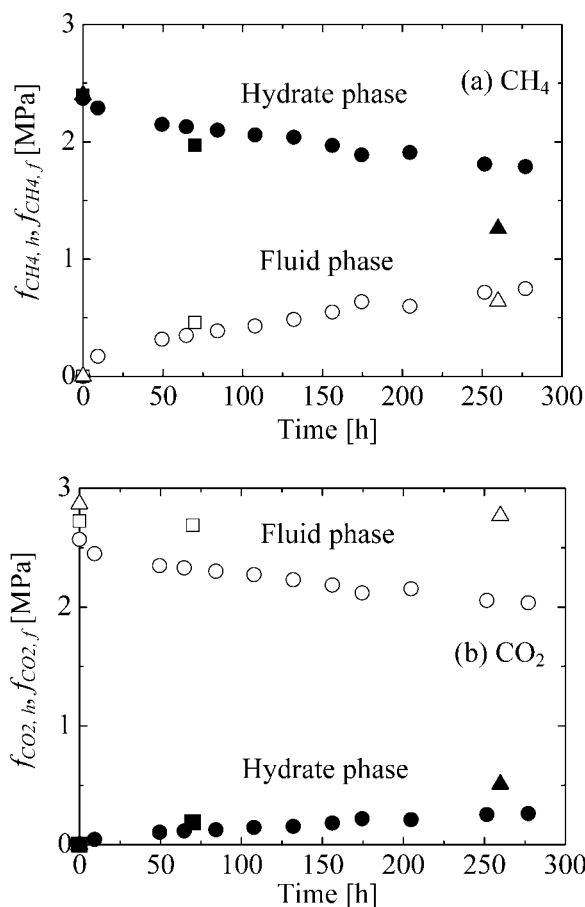


**Figure 2.** Fugacity of each component of the fluid phase (white symbol) and hydrate phase (filled symbol) during the replacements in batch experiments as a function of time at 273.2 K and initial pressures of 3.26 MPa (circles), 5.40 MPa (squares), and 6.00 MPa (triangles): (a) CH<sub>4</sub>, (b) CO<sub>2</sub>.

with time. Considering the effect of  $f_{CO_2,f}$  on the replacement rates obtained in Figure 1, it can be seen that replacement rates increased with increasing  $f_{CO_2,f}$ . The almost constant replacement rates at 5.40 and 6.00 MPa (Figure 1) seem to correspond to the fluid fugacity in the liquid-hydrate reaction (Figure 2b). For examining the relationship between the driving force of the replacement and the fugacity, the absolute fugacity difference of each component between the fluid and hydrate phases ( $\Delta f_{CH_4}$ ,  $\Delta f_{CO_2}$ ) were plotted against time (Figure 3). As shown in Figure 3, the  $\Delta f_{CH_4}$  and  $\Delta f_{CO_2}$  decreased with time, however, the  $\Delta f_{CO_2}$  at 5.40 and 6.00 MPa were smaller than the corresponding values at 3.26 MPa, while  $\Delta f_{CO_2}$  at 5.40 and 6.00 MPa were larger than those at 3.26 MPa. The larger  $\Delta f_{CO_2}$  probably lead to faster replacement and helped to explain the larger slope for  $\Delta f_{CH_4}$ . Replacement rates seemed to be directly related to component fugacity differences, especially for CO<sub>2</sub>, and, from these results, it is probable that the replacement rates can be promoted by increasing the CO<sub>2</sub> fugacity.

### Microscopic mechanism of CH<sub>4</sub>-CO<sub>2</sub> replacement in the hydrate phase (Run 4)

In this work, we calculated fractional cage occupancies using the van der Waals-Platteeuw theory (CSMHYD program<sup>1</sup>) through the continuous measurement data of cage decompositions during replacement. Raman spectra of CH<sub>4</sub> hydrate under high pressure CO<sub>2</sub> gas atmosphere obtained before the replacement reaction are shown in Figure 4. Symmetric C—H stretching of CH<sub>4</sub> in the M-cage and the S-cage was found at 2905 and 2915 cm<sup>-1</sup>, respectively, showing good agreement with literature values.<sup>17,18</sup> The Raman peak of the symmetric C—H stretching of CH<sub>4</sub> in the gas phase (2917 cm<sup>-1</sup>) is also shown in Figure 4. When we measured the Raman spectra of the CH<sub>4</sub> hydrate under a CH<sub>4</sub> gas atmosphere, the Raman peak of gaseous phase overlapped with that of the hydrate phase. In our experiments, CO<sub>2</sub> gas was flowed through the cell during the replacement to minimize the effect of CH<sub>4</sub> gas contribution to the CH<sub>4</sub> hydrate Raman spectra.

In the analysis of the Raman spectra for the remaining CH<sub>4</sub> hydrate, the obtained peak areas were divided into S-cage

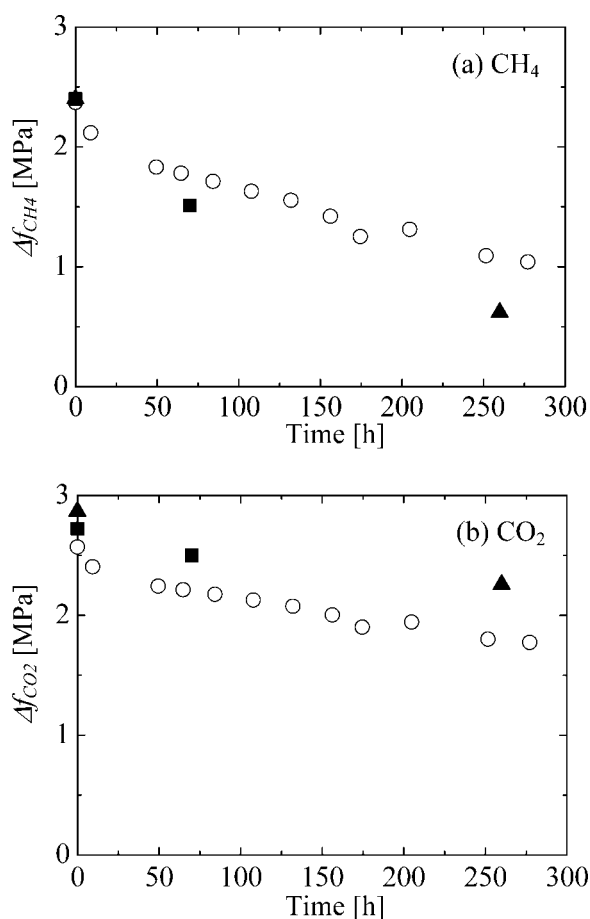


**Figure 3.** Fugacity differences of CH<sub>4</sub> and CO<sub>2</sub> between fluid and hydrate phase in batch reactions as a function of time at 273.2 K and initial pressures of 3.26 MPa (circles), 5.40 MPa (squares), and 6.00 MPa (triangles): (a) CH<sub>4</sub>, (b) CO<sub>2</sub>.

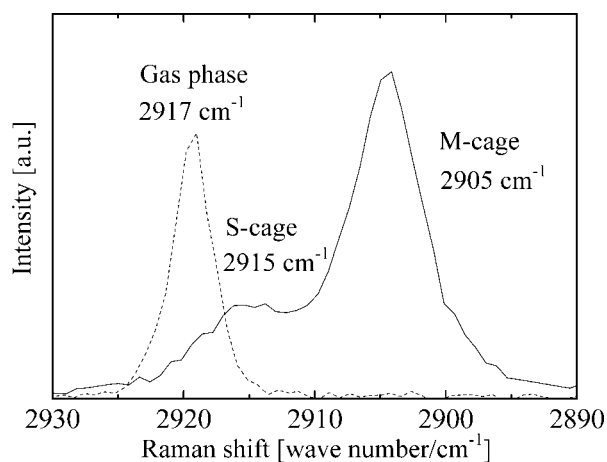


**Figure 4.** Raman spectra of CH<sub>4</sub> hydrate showing symmetric C–H stretching of CH<sub>4</sub> in the M-cage and S-cage at 2905 and 2915 cm<sup>−1</sup>, respectively, and (continuous line) and that in the gas phase at 2917 cm<sup>−1</sup> (dashed line).

and M-cage by deconvolution assuming Gaussian–Lorentzian bands. The M-cage/S-cage ratios (M/S cage ratios) were calculated with the area of each assigned peak. The time evolution of the Raman spectra of CH<sub>4</sub> hydrate (raw data) and calculated M/S ratios in CH<sub>4</sub> hydrate are shown in Figures 5 and 6, respectively. In Figure 6, the M/S ratio decreased almost linearly with time, which means that the decomposition of the M-cage was faster than that of the S-cage during the replacement, which is in agreement with our previous findings.<sup>9</sup> From the obtained data in this work and the previous report,<sup>9</sup> faster decomposition of M-cage than S-cage in the CH<sub>4</sub> hydrate can be concluded for both liquid and gaseous CO<sub>2</sub>.

To understand the difference in decomposition rates between the M-cage and the S-cage, the related fractional occupancy of each cage ( $\theta_{M,CH_4}$ ,  $\theta_{S,CH_4}$ ) in the CH<sub>4</sub> hydrate

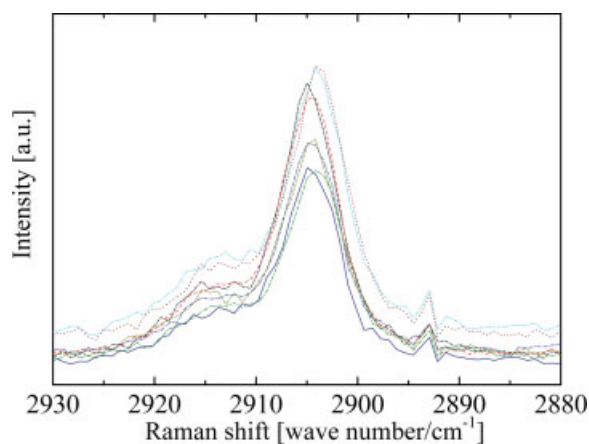


**Figure 5.** Time evolution for Raman spectra of CH<sub>4</sub> hydrate during replacement (raw data).

[Color figure can be viewed in the online issue, which is available at [www.interscience.wiley.com](http://www.interscience.wiley.com).]

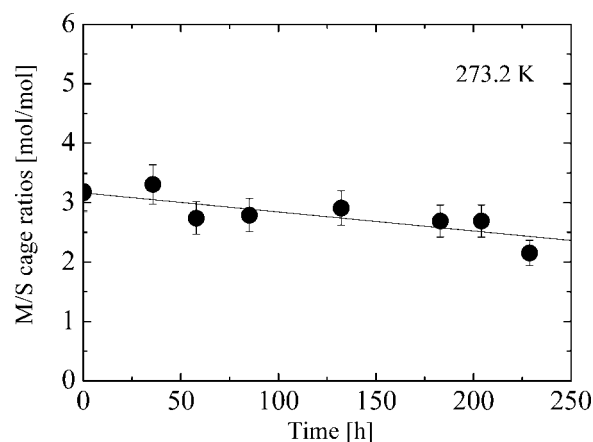


**Figure 6.** Molar ratio of cage decompositions between M-cage and S-cage (M/S cage ratios) obtained by the Raman analysis of CH<sub>4</sub> hydrate in the flow experiment (Run 4) as a function of time at 273.2 K and the initial pressure of 3.20 MPa.

was estimated with the van der Waals–Platteeuw model, since the occupancies of the cavities could not be estimated from the Raman spectra of CH<sub>4</sub> hydrate directly. If the occupancies of the cages were considered as quasi-equilibrium values, they can be theoretically determined from the experimental conditions ( $T$ ,  $P$ ,  $h_{CH_4}$ ,  $h_{CO_2}$ ) that were available from quantitative analyses of the batch experiments.

In the calculation, we chose the temperature to be 273.2 K and the initial pressure to be 3.26 MPa that matches the gaseous–hydrate reaction in Run 1, and which was considerably close to the conditions of 273.2 K and 3.20 MPa for measurements of M/S cage ratios in Run 4. We calculated the occupancy of each cage for Run 1 with the van der Waals–Platteeuw theory as shown in Figure 7.

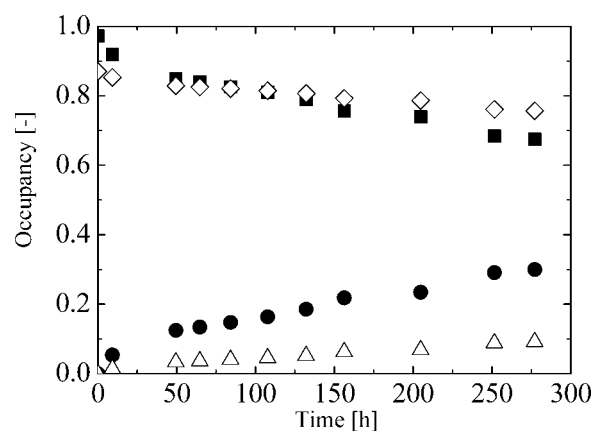


**Figure 7.** Fractional occupancies of M-cage and S-cage calculated with the van der Waals–Platteeuw theory using the changes of compositions of the hydrate phase in the batch experiment (Run 1) as a function of time at 273.2 K:  $\theta_{M,CH_4}$  (squares),  $\theta_{S,CH_4}$  (diamonds),  $\theta_{M,CO_2}$  (circles), and  $\theta_{S,CO_2}$  (triangles).

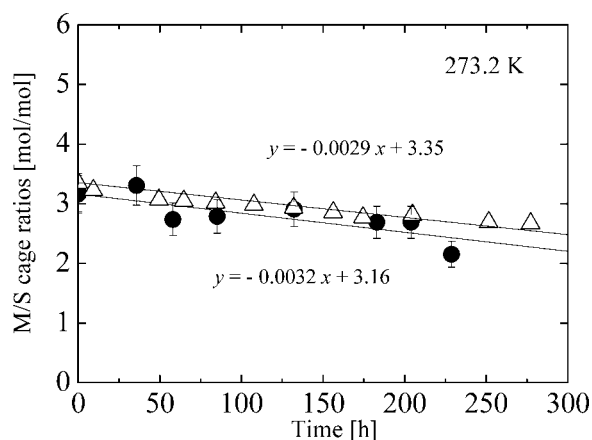


**Figure 8.** Comparison of the M/S cage ratios measured by the in-situ Raman technique in Run 4 (circles) with the theoretical value calculated by the van der Waals–Platteeuw theory (triangles) using the composition of the hydrate phase quantified in the batch experiment (Run 1) at 273.2 K.

For  $\text{CH}_4$  hydrate decomposition during replacement, the occupancy of M-cage in  $\text{CH}_4$  hydrate ( $\theta_{\text{M,CH}_4}$ ) decreased much faster than  $\text{CH}_4$  occupancy in the S-cage ( $\theta_{\text{S,CH}_4}$ ) with time. For  $\text{CO}_2$  hydrate formation,  $\theta_{\text{M,CO}_2}$  also increased much faster than  $\theta_{\text{S,CO}_2}$  for the period studied. These findings show that the replacement seemed to mainly occur in the M-cage.

On the other hand, both the decreasing rate of  $\text{CH}_4$  occupancies and the increasing rate of  $\text{CO}_2$  occupancies were much larger at the early stages ( $\sim 10$  h) than those at the latter stages. From available data in the literature and experiments performed in our previous work,<sup>8</sup> it seemed that in the initial stage, the surface area available to the bulk gas changed greatly as the reaction proceeded. Therefore, the faster replacement at the early stage can probably be explained as a rapid surface reaction.

The theoretical M/S cage ratios can be calculated from the following equation:

$$\text{M/S cage ratios} = N_{\text{M}}\theta_{\text{M,CH}_4}/N_{\text{S}}\theta_{\text{M,CH}_4} \quad (1)$$

where  $N_{\text{M}}$  and  $N_{\text{S}}$  are the number of M-cage ( $N_{\text{M}} = 6$ ) and S-cage ( $N_{\text{S}} = 2$ ) in the unit cell of sI hydrate and  $\theta$  is the fractional occupancies as before. Comparison between the M/S cage ratio in the  $\text{CH}_4$  hydrate calculated theoretically and that obtained by Raman analysis is shown in Figure 8. The slopes of the M/S cage ratios determined by the two methods were close and seemed to confirm agreement between the in-situ Raman measurements and calculations with Eq. 1.

The phenomenon of faster decomposition of M-cage in the  $\text{CH}_4$  hydrate during the replacement can be interpreted as follows. One of the possible reasons for the rate difference is the higher stability of  $\text{CH}_4$  in the S-cage than in the M-cage, which can be attributed to the smaller strain of the S-cage for  $\text{CH}_4$  compared with the M-cage.<sup>18</sup> Considering from the activation energy ( $\Delta E_{\text{A}}$ ) of replacement in our previous study,<sup>8</sup>  $\Delta E_{\text{A}}$  for  $\text{CH}_4$  hydrate decomposition was practically identical to the decomposition enthalpy of  $\text{CH}_4$  hydrate to

ice and gas. This implies that the decomposition of both M- and S-cages occurred simultaneously, although there could be some influence on the decomposition rates due to the difference in M- and S-cage stability. The other possible reason could be the reformation of the S-cage occupying some portion of released  $\text{CH}_4$  during the replacement in the M-cage, because  $\text{CO}_2$  molecules hardly occupy the S-cage due to the balance between molecular diameter and cavity size.<sup>1</sup> The kinetic model proposed for the microscopic replacement for the assumption of reformation of the  $\text{CH}_4$  released from the S-cage was found to correlate fairly well with the time evolution of  $\text{CH}_4$  remaining in the hydrate phase.<sup>9</sup> This means that the reformed S-cage might involve some portion of the released  $\text{CH}_4$ , which induced the apparent reduction of the S-cage decomposition rate. This phenomenon might be related to the rates of intrinsic cage formation of M- and S-cages<sup>19,20</sup> and the memory effect of the hydrogen bonds<sup>21–23</sup> as well.

Moudrakovski et al. suggested that the formation of the S-cage was faster than that of the M-cage from  $^{129}\text{Xe}$  NMR analysis of the xenon hydrate.<sup>19</sup> A similar result was reported for  $\text{CH}_4$  hydrate formation by the Raman analysis.<sup>20</sup> During the replacement, this faster formation of the S-cage might lead to the  $\text{CH}_4$  reoccupation in the S-cage when the replacement occurs in the M-cage.

On the other hand, Takeya et al.<sup>21</sup> suggested that nucleation rates of  $\text{CO}_2$  hydrate with melt water from ice were larger than those for nonfrozen water. They called this phenomenon the freezing-memory effect on nucleation. Komai et al. suggested that the repetition of the hydrate formation and decomposition could lead to a decrease in hydrate formation pressure of the hydrate,<sup>6</sup> namely, the iteration of this process makes hydrate formation easier, suggesting that memory effects of hydrogen bonds exist. Buchanan et al. examined the water structure before the  $\text{CH}_4$  hydrate growth and after hydrate decomposition using neutron diffraction analysis.<sup>22</sup> They suggested that there was no significant difference between the structure of water before the hydrate formation and that after the hydrate decomposition. In their analysis, they confirmed the existence of the memory effect in individual  $\text{CH}_4$  hydrate. These reports suggest the contribution of some memory effect of hydrogen bonds in hydrate formation.

It can be concluded that the guest molecule replacement in the hydrate phase starts with decomposing the cages in the  $\text{CH}_4$  hydrate, which is induced by the diffusion of  $\text{CO}_2$  molecules into the hydrate phase with a driving force of its fluid fugacity. Then, the memory effect of the hydrogen bonds probably helps to restructure the S-cage and leads to the reoccupation of some portion of  $\text{CH}_4$  in the S-cages, where the  $\text{CO}_2$  molecules have low occupancy,<sup>5</sup> and consequently, the replacement mainly proceeds in M-cages.

## Conclusions

We investigated the effects of pressure and fugacity on the  $\text{CH}_4$ – $\text{CO}_2$  replacement in  $\text{CH}_4$  hydrate using quantitative analysis with in-situ laser Raman spectroscopy. It was found that the  $\text{CH}_4$ – $\text{CO}_2$  replacement at the boundary of liquid and hydrate phase (273.2 K and above 3.60 MPa) proceeds faster than that at the boundary of gaseous and hydrate phase (273.2 K and 3.26 MPa). For the replacement in the liquid phase, pressure dependence was hardly observed at condi-

tions studied. The fugacity differences between the fluid and the hydrate phases were found to be effective for describing the driving force of CH<sub>4</sub>–CO<sub>2</sub> replacement. Raman analysis of the hydrate phase during the CH<sub>4</sub>–CO<sub>2</sub> replacement revealed faster decomposition of M-cage than S-cage. Estimation with the van der Waals–Platteeuw theory was applied to the available data and supported the experimental findings. From this approach, occupancies of CH<sub>4</sub> in each cage could be estimated during replacement process. In the future, the estimation of CO<sub>2</sub> occupancies, which could not be obtained directly from the Raman analysis, would be desirable. It would also be desirable to determine the surface area of the hydrate under conditions in this work using in-situ techniques such as the focused beam reflectance method proposed by Clarke and Bishnoi<sup>23</sup> and to elucidate the intrinsic rate constant for the replacement processes.

## Literature Cited

1. Sloan ED. *Clathrate Hydrates of Natural Gases*, 2nd edition. New York, NY: Marcel Dekker, 1998.
2. Ohgaki K, Takano K, Moritoki M. Exploitation of CH<sub>4</sub> hydrates under the NANKAI TROUGH in combination with CO<sub>2</sub> storage. *Kagaku Kogaku Ronbun*. 1994;20:121–123.
3. Ohgaki K, Sangawa H, Matsubara T, Nakano S. Methane exploitation by carbon dioxide from gas hydrates—phase equilibria for CO<sub>2</sub>–CH<sub>4</sub> mixed hydrate system. *J Chem Eng Jpn*. 1996;29:478–483.
4. Yezdimer EM, Cummings PT, Chialvo AA. Determination of the Gibbs free energy of gas replacement in SI clathrate hydrates by molecular simulation. *J Phys Chem A* 2002;106:7982–7987.
5. Hirohama S, Shimoyama Y, Wakabayashi A, Tatsuta S, Nishida N. Conversion of CH<sub>4</sub>-hydrate to CO<sub>2</sub>-hydrate in liquid CO<sub>2</sub>. *J Chem Eng Jpn*. 1996;29:1014–1020.
6. Komai T, Kawamura T, Kang S, Nagashima K, Yamamoto Y. In situ observation of gas hydrate behavior under high pressure by Raman spectroscopy. *J Phys: Condens Matter* 2002;14:11395–11400.
7. Yoon JH, Kawamura T, Yamamoto Y, Komai T. Transformation of methane hydrate to carbon dioxide hydrate: in situ Raman spectroscopic observations. *J Phys Chem A* 2004;108:5057–5059.
8. Ota M, Abe Y, Watanabe M, Smith RL, Inomata H. Methane recovery from methane hydrate using pressurized CO<sub>2</sub>. *Fluid Phase Equilib*. 2005;228/229:553–559.
9. Ota M, Morohashi K, Abe Y, Watanabe M, Smith RL, Inomata H. Replacement of CH<sub>4</sub> in the hydrate by use of liquid CO<sub>2</sub>. *Energ Convers Manage*. 2005;46:1680–1691.
10. Clarke MA, Bishnoi PR. Determination of the intrinsic kinetics of CO<sub>2</sub> gas hydrate formation using in situ particle size analysis. *Chem Eng Sci*. 2005;60:695–709.
11. Svandal A, Kvamme B, Grønås L, Pusztai T, Buanes T, Hove J. The phase-field theory applied to CO<sub>2</sub> and CH<sub>4</sub> hydrate. *J Cryst Growth* 2006;287:486–490.
12. Sum AK, Burruss RC, Sloan ED. Measurement of clathrate hydrates via Raman spectroscopy. *J Phys Chem B* 1997;101:7371–7377.
13. Lee H, Seo Y, Seo YT, Moudrakovski IL, Ripmeester JA. Recovering methane from solid methane hydrate with carbon dioxide. *Angew Chem Int Ed*. 2003;42:5048–5051.
14. van der Waals JH, Platteeuw JC. Clathrate Solutions. *Adv Chem Phys*. 1959;2:1–57.
15. Trebble MA, Bishnoi PR. Development of a new 4-parameter cubic equation of state. *Fluid Phase Equilib*. 1987;35:1–18.
16. Soave G. Equilibrium constants from a modified Redlich–Kwong equation of state. *Chem Eng Sci*. 1972;27:1197–1203.
17. Uchida T, Takeya S, Wilson LD, Tulk CA, Ripmeester JA, Nagao J, Ebinuma T, Narita H. Measurements of physical properties of gas hydrates and in situ observations of formation and decomposition processes via Raman spectroscopy and X-ray diffraction. *Can J Phys*. 2003;81:351–357.
18. Subramanian S, Sloan ED. Microscopic measurements and modeling of hydrate formation kinetics. *Ann N Y Acad Sci*. 2000;912:583–592.
19. Moudrakovski IL, Snachez AA, Ratcliffe CI, Ripmeester JA. Nucleation and growth of hydrates on ice surfaces: New insights from Xe-129 NMR experiments with hyperpolarized xenon. *J Phys Chem B* 2001;105:12338–12347.
20. Uchida T, Okabe R, Mae S, Ebinuma T, Narita H. In situ observation of methane hydrate formation mechanisms by Raman spectroscopy. *Ann N Y Acad Sci* 2000;912:593–601.
21. Takeya S, Hori A, Hondoh T, Uchida T. Freezing memory effect of water on nucleation of CO<sub>2</sub> hydrate crystals. *J Phys Chem B* 2000;104:4164–4168.
22. Buchanan P, Soper AK, Thompson H, Westacott RE, Creek JL, Hobson G, Koh CA. Search for memory effects in methane hydrate: structure of water before hydrate formation and after hydrate decomposition. *J Chem Phys*. 2005;123:164507.
23. Clarke M, Bishnoi PR. Determination of the intrinsic rate constant and activation energy of CO<sub>2</sub> gas hydrate decomposition using in situ particle size analysis. *Chem Eng Sci*. 2004;59:2983–2993.

Manuscript received Sept. 27, 2006, and revision received July 31, 2007.